

Absorber Intercooling in CO₂ Absorption by Piperazine-Promoted Potassium Carbonate

Jorge M. Plaza, Eric Chen, and Gary T. Rochelle

Dept. of Chemical Engineering, The University of Texas at Austin, Austin, TX 78712

DOI 10.1002/aic.12041

Published online November 5, 2009 in Wiley InterScience (www.interscience.wiley.com).

Intercooling was evaluated as a process option in CO₂ absorption by piperazine (PZ) promoted potassium carbonate. The system performance with 4.5 m K⁺/4.5 m PZ was simulated by a model in Aspen Plus® RateSep™. The absorber was evaluated for use with a double matrix stripper by optimizing the position of the semilean feed and intercooling stages to maximize CO₂ removal. Additionally, a simple absorber system was modeled to observe the effect of intercooling on systems with variable CO₂ lean loading. Intercooling increases CO₂ removal by as much as 10% with the double matrix configuration. With a simple absorber, the effectiveness of intercooling depends on solvent rate. Near a critical liquid/gas ratio (L/G) there is a large improvement with intercooling. This is related to the position of the temperature bulge. An approximation is proposed to estimate the critical L/G where intercooling may maximize removal. © 2009 American Institute of Chemical Engineers *AIChE J*, 56: 905–914, 2010

Keywords: CO₂ absorption, temperature bulge, modeling, intercooling, critical L/G

Introduction

Carbon dioxide capture and sequestration is a major option to reduce greenhouse gases and address global climate change. Chemical absorption is the most attractive technology to reduce CO₂ emissions from coal fired plants.

Intercooling is a common strategy to increase the performance of absorption systems. Jackson and Sherwood¹ showed that intercooling increased absorption up to 37% and even higher during the winter in refinery gas absorbers for absorption of C₄⁺ from cracking coal gas. Linhoff² reports the use of intercooling in a refinery with vapor recovery by an absorption oil. Sobel³ introduces the use of a computational method for absorbers which routinely include a feature for modeling intercooling. A number of authors have shown that absorber intercooling can be effective with CO₂ capture by amines.^{4–7} Patents have also been filed with more complex intercooling configurations to increase absorber performance.^{8–10}

Intercooling is especially useful for systems where the heat of absorption (i.e., heat of solution and/or reaction) results in

an increase in temperature of the solvent affecting the vapor pressure of the dissolved species. Kvamsdal and Rochelle¹¹ observed this behavior for the absorption of carbon dioxide from flue gas by aqueous monoethanolamine (MEA). They studied absorber parameters such as liquid/gas ratio (L/G), height of packing, and flue gas composition and its effect on the appearance of a temperature bulge in the absorber. Chen¹² observed similar behavior for systems using piperazine- (PZ) promoted potassium carbonate (K⁺). He developed a rate-based absorber model for the mentioned system. The model was originally generated from work carried out by Cullinane¹³ and later translated into Aspen Plus® by Hillard.¹⁴ Chen used the Data Regression System® in Aspen Plus® to simultaneously regress equilibrium constants and interaction parameters to predict equilibrium and speciation.

This work uses the tools developed by Chen to analyze a system using a 4.5 m K⁺/4.5 m PZ solvent. Different absorber configurations were studied to evaluate the effect of intercooling on absorber performance.

Vapor-Liquid Equilibrium (VLE) and Kinetics Model

The K⁺/PZ solvent was introduced by Cullinane¹³ as an alternative to the widely used MEA. MEA has a high

Correspondence concerning this article should be addressed to G. T. Rochelle at Rochelle@che.utexas.edu

Table 1. Activity-Based Rate Parameters for Formation of PZCOO^- in 4.5 m K^+ /4.5 m PZ

b*	Forward			Reverse		
	$k \times 10^{10}$	E (kJ/kmol)	n	k	E (kJ/kmol)	n
OH^-	28.11	-67,847	34.75	2.12×10^{-2}	246,966	-38.02
H_2O	0.0127	-42,414	23.48	2.93×10^{12}	160,611	-26.81
PZ	3.25	-155,841	53.66	6.12×10^2	325,276	-66.41
CO_3^{2-}	17.64	-105,880	53.25	3.42×10^3	200,502	-32.53
PZCOO^-	10.40	-51,821	28.72	6.12×10^2	325,276	-66.41

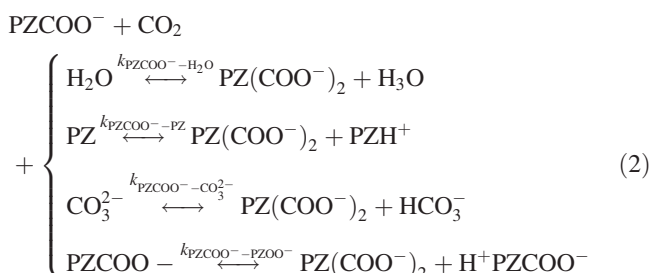
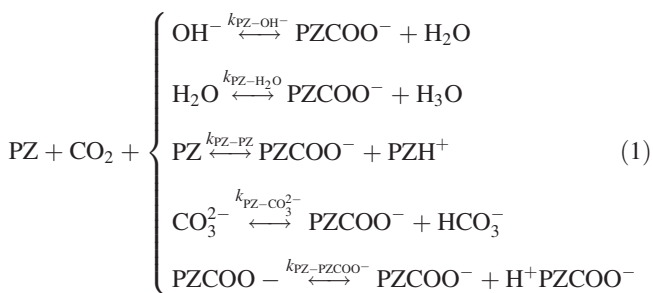
*b corresponds to $\text{PZ} + \text{CO}_2 + \text{b} \leftrightarrow \text{PZCOO}^- + \text{bH}^+$

capacity and a fast rate of CO_2 absorption. According to Cullinane, the K^+ /PZ solvent has a higher CO_2 capacity than MEA because PZ is a diamine and potassium carbonate increases the absorption capacity. Furthermore, the rate of absorption was increased due to the presence of two amine groups in PZ, the high pK_a , and the large quantity of carbonate/bicarbonate. He reported a CO_2 absorption rate 1.5 to three times faster than with 30 wt % MEA.

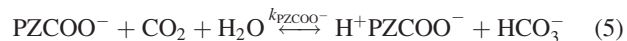
Cullinane¹³ measured the thermodynamics and kinetics of potassium carbonate, piperazine, and carbon dioxide using a wetted wall column and developed a rigorous thermodynamic model in FORTRAN using the electrolyte nonrandom two-liquid (e-NRTL) theory. The model predicted vapor–liquid equilibrium (VLE) and speciation for the $\text{H}_2\text{O}-\text{K}_2\text{CO}_3-\text{PZ}-\text{CO}_2$ system. The equilibrium constants and interaction parameters were regressed using experimental data and input into the FORTRAN model. Additionally, a rigorous kinetic model was developed that determined the rate constants and diffusion coefficients based on experimental data.

Cullinane conducted experiments with 0.45–3.6 m PZ and 0–3.1 m potassium carbonate at 25–110°C. The absorption rate of CO_2 was determined using the eddy diffusivity model developed by Bishnoi and Rochelle¹⁵ and rate constants were regressed from the experimental data using the model. The reaction of CO_2 with piperazine was modeled with a termolecular, base-catalyzed mechanism.

The following amine reactions were used in the Cullinane¹³ model.



All of the buffering reactions were considered to be in equilibrium and reversible rate expressions for CO_2 with PZ and PZCOO^- were developed. The catalysis of the formation of bicarbonate ion by hydroxide, piperazine, and piperazine carbamate was also included in the Cullinane model. The reactions to form bicarbonate ion were included to properly model equilibrium in the boundary layer and do not affect the CO_2 absorption rate. The three reversible reactions are:



Hilliard¹⁴ developed a VLE model in Aspen Plus® using the thermodynamic data by Cullinane and the Data Regression System® (DRS) to simultaneously regress the interaction parameters and equilibrium constants to be used in the built-in electrolyte-NRTL model.

Later, Chen¹² developed a rate-based model using Aspen Plus® RateSep™. It incorporates the Hilliard VLE model to predict equilibrium and speciation, and the rate constants developed by Cullinane to predict kinetics. The model calculates heat and mass transfer using Onda¹⁶ and the Chilton–Colburn Analogy and physical properties using correlations specified by the user within the Aspen Plus® framework.

Initial absorber modeling by Chen predicted an unexpected temperature profile indicating that the heat of absorption for CO_2 was not being correctly predicted by Aspen Plus®. This was in part due to the fact that the simultaneous regression of the interactions parameters by Hilliard did not incorporate heat capacity data for the $\text{K}_2\text{CO}_3-\text{PZ}-\text{CO}_2-\text{H}_2\text{O}$ system. Therefore, the temperature dependence of the regressed binary interaction and enthalpy parameters may not have been adequately captured.

The heat of absorption calculated by Aspen Plus® is derived from an enthalpy balance using the heats of formation, heat capacities, and heats of vaporization of the various species. The heats of formation of the piperazine species (PZH^+ , PZCOO^- , $\text{PZ}(\text{COO}^-)_2$, and H^+PZCOO^-) were adjusted to provide the same heat of CO_2 absorption as that predicted from equilibrium constants used in the chemistry model. The heats of formation (liquid) at 298.15 K were calculated using the parameters from the equilibrium constants and the Van't Hoff equation. The equilibrium equations and results obtained for the four piperazine species can be found in Chen.¹²

Table 2. Activity-Based Rate Parameters Formation of PZ(COO⁻)₂ in 4.5 m K⁺/4.5 m PZ

b*	Forward			Reverse		
	k × 10 ¹²	E (kJ/kmol)	n	k	E (kJ/kmol)	n
H ₂ O	0.0039	61,606	-1.46	2.22 × 10 ¹³	78,135	-1.46
PZ	2.02	-51,821	28.72	9.45 × 10 ³	242,800	-41.06
CO ₃ ⁻²	5.39	-1,860	28.31	2.59 × 10 ⁴	118,027	-7.18
PZCOO ⁻	0.0065	52,199	3.78	2.07 × 10 ⁴	116,084	3.78

*b corresponds to PZCOO⁻ + CO₂ + b ↔ PZ(COO⁻)₂ + bH⁺

As the Hilliard VLE model does not contain heat capacity parameters for the PZ species [(PZH⁺, PZCOO⁻, PZ(COO⁻)₂, H⁺PZCOO⁻)] regressed entropy reference values for the four PZ species were used to calculate heat capacities. Multiparameter heat capacity correlations were developed using the equilibrium constants. Aspen Plus[®] does not account for the existence of net-neutrally charged zwitterions which were included in the Hilliard K⁺/PZ VLE model. The H⁺PZCOO⁻ ion was given a net charge of 0 and was thus treated as a molecule. This created a number of issues such as the skewed predictions of the heats of absorption. Therefore, the charge for the H⁺PZCOO⁻ ion was changed to 0.0001.

The equilibrium constants were activity-based while the rate constants developed by Cullinane used concentration-based units. Therefore, Chen implemented activity-based kinetics within the model, taking advantage of the fact that the new version of RateSepTM has the capability to handle activities, in terms of mole gamma, using the power law kinetic expression:

$$r = k \left(\frac{T}{T_0} \right)^n \exp \left(\frac{-E}{R} \left(\frac{1}{T} - \frac{1}{T_0} \right) \right) \prod (x_i \gamma_i)^{\alpha_i} \quad (6)$$

where *k* is the pre-exponential factor (independent of temperature), *n* is the temperature exponent, *E* is the activation energy, *T*₀ is the reference temperature (298.15 K), *x_i* is the fraction of reactant species *i*, γ_i is the activity coefficient, and α_i is the reaction order for the species.

A simple algebraic manipulation was performed using the following equation:

$$k_a = \frac{k_c [PZ][CO_2][b]}{(x_{PZ}\gamma_{PZ})(x_{CO_2}\gamma_{CO_2})(x_b\gamma_b)(\text{total mol/L})} \quad (7)$$

where *k_a* is the activity-based rate constant, *k_c* is the concentration-based rate constant, [b] is the concentration of species b in units of mol/L, and *x_b* is the mole fraction and γ_b is the activity coefficient. The last term in the denominator represents the total molar concentration per liter of solvent and will be specific for a particular solvent composition and

loading. Therefore, a representative total molar concentration was selected and assumed to be constant across the column.

Kinetics developed by Cullinane contain a correction for ionic strength. However, in Aspen Plus[®], this correction cannot be directly implemented. Therefore, a representative ionic strength at 50°C and 0.5 loading (mol CO₂/total alkalinity) was selected over the temperature and loading range of this study (the calculated ionic strength varied less than 5%).

Chen¹² reported results for the forward and reverse activity-based rate parameters for piperazine, piperazine carbamate, and bicarbonate reactions as input into Aspen Plus[®] RateSepTM for systems with 5 m K⁺/2.5 m PZ, 6.4 m K⁺/1.6 m PZ. The power law constants for the 4.5 m K⁺/4.5 m PZ, were calculated using the methodology used by Chen and are presented in Tables 1–3.

The absorber was simulated with a rate-based model accounting for mass transfer resistance and reaction kinetics. Kinetics, in the liquid film, were calculated by discretizing it into five segments with a ratio of 10 for the first four segments starting at 0.0001 and a value of 0.4 for the segment closest to the bulk liquid. Electrolyte thermodynamics were also considered. This approach required a full characterization of mass and heat transfer, hydrodynamics, vapor–liquid equilibrium, and physical properties of the entire system. This model was set up in Aspen Plus[®] using RateSepTM. The previously obtained activity-based kinetics were introduced along with the VLE model generated by Hilliard.¹⁴ Packing interfacial area was calculated using the built-in correlation in Aspen by Onda¹⁶

The developed model was used to evaluate the effect of solvent loading and intercooling on the performance of the absorber. The absorber was modeled with 15 m of packing divided into 30 calculation stages. Table 4 shows the absorber design specifications. Table 5 shows the conditions of the gas feed stream.

The Double Matrix System

Oyenekan¹⁷ proposed a stripper configuration for the regeneration of the solvent for the absorption of CO₂ that reduces the temperature change across the stripper by using

Table 3. Activity-Based Rate Parameters for the Formation of HCO₃⁻ in 4.5 m K⁺/4.5 m PZ

a*	b*	Forward			Reverse		
		k × 10 ¹²	E (kJ/kmol)	n	k	E (kJ/kmol)	n
-	OH ⁻	5.28 × 10 ⁻⁶	54,758	5.24	2.18 × 10 ⁻³	66,014	19.54
H ₂ O	PZ	2.27 × 10 ⁻⁸	-30,856	24.15	2.35	146,702	-8.85
H ₂ O	PZCOO ⁻	1.04 × 10 ⁻⁸	73,163	-0.79	7.39	19,986	35.99

*a, b correspond to a + CO₂ + b ↔ HCO₃⁻ + bH⁺. (OH⁻ does not form bH⁺).

Table 4. Absorber Design Conditions for Most Modeling Cases

Variable	Value
Diameter (m)	9.8
Height (m)	15.0
Packing Characteristics	
Type	CMR
Vendor	MTL
Material	Metal
Dimension	NO-2P
Liquid hold up (%)	5

a multipressure system (see Figure 1). The rich solution from the absorber is split into two streams: one goes to a higher pressure stripper while the other goes to a lower pressure stripper. This configuration generates two return streams to the absorber (lean and semilean). Depending on the operating condition, these streams will be at higher or lower loading and their flow will also vary.

Van Wagener,¹⁸ based on the work by Oyenekan, modeled the double matrix configuration using the 4.5 m K⁺/4.5 m PZ solvent. Results from this analysis provided an optimum loading (moles of CO₂/moles of alkalinity) of 0.4012 for the lean stream and 0.4598 for the semilean stream. The flow split between the streams was 0.1850 (mol semilean/mol lean). These values correspond to 0.5 kPa partial pressure of CO₂ in the lean stream at 40°C. These data were used to set up an absorber optimization to maximize CO₂ removal using a fixed packing height and varying the position of the semilean feed and an additional intercooling point. Figure 2 summarizes the conditions used for this analysis.

Figure 3 demonstrates optimization of the case using a semilean feed without intercooling. The position of the semilean feed was adjusted to maximize CO₂ removal. Removal is not very sensitive to the feed position, but an optimum is found 30% from the top. Figure 4 gives the resulting liquid temperature and CO₂ rate profile.

Intercooling was defined to achieve 40°C at the selected stage, which should be feasible with cooling water. When intercooling was used at the same point as the semilean feed, the optimum semilean feed position changed from the upper half of the column to the lower third. (See Figures 5 and 6.)

Figure 7 shows the profiles obtained with an additional intercooling stage. The semilean feed with intercooling was simultaneously optimized along with the additional intercooling point. The optimum locations for the semilean and the additional intercooling were found at 0.63 and 0.87 of the column height, respectively.

Table 5. Flue Gas Conditions Used for Simulation Cases

Variable	Value
Flow (kmol/s)	5.4879
Temperature (°C)	40.0
Pressure (kPa)	111.33
Mol fraction	
H ₂ O	0.0670
CO ₂	0.1270
N ₂	0.7569
O ₂	0.0491

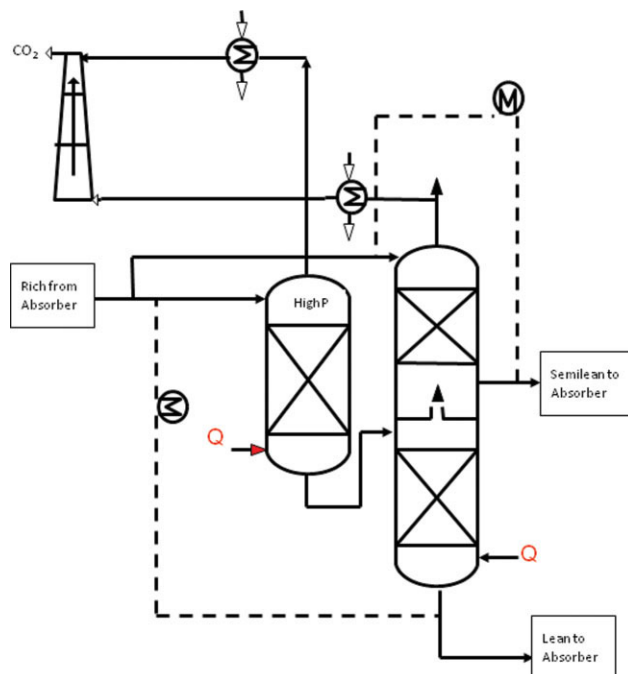


Figure 1. Double matrix stripper configuration.

[Color figure can be viewed in the online issue, which is available at www.interscience.wiley.com.]

Van Wagener reported conditions for the stripper using a higher loading lean solvent corresponding to 0.7 kPa CO₂ partial pressure. The lean solvent loading was 0.4208, the semilean loading was 0.4743 and the split was 0.1453. An analysis analogous to the 0.5 kPa loading was conducted, obtaining similar results. A summary of the results for the various operating conditions modeled is presented in Table 6. A single intercooling at the point of the semilean feed is very effective. Additional intercooling provides only marginal improvement.

Effect of Intercooling on Solvent Capacity and Rich Loading

The lean solvent loading was varied to determine its effect on solvent capacity and rich loading for a simple absorber system with a single feed while maintaining removal at 90%. Solvent capacity is defined as the kmol of CO₂ removed per kg lean solvent feed.

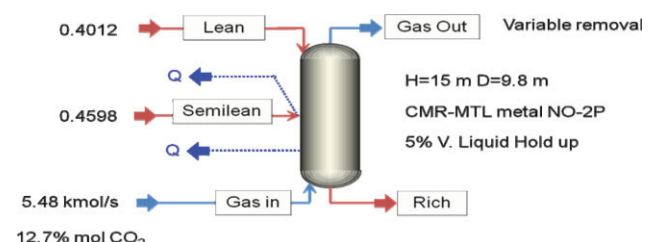


Figure 2. Absorber modeling conditions for 4.5 m/4.5 m K⁺/PZ.

[Color figure can be viewed in the online issue, which is available at www.interscience.wiley.com.]

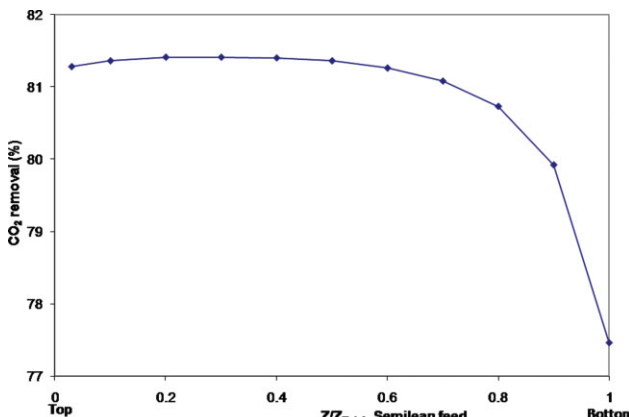


Figure 3. CO_2 removal with semilean feed with no intercooling for the 4.5 m/4.5 m K^+/PZ system.

0.5 kPa CO_2 lean solvent, 15 m packing. [Color figure can be viewed in the online issue, which is available at www.interscience.wiley.com.]

Intercooling was set up in a similar matter to the previous analysis. It was placed in the middle of the column and at the optimum point (minimum amount of solvent for the level of lean loading). The flue gas and absorber specifications are the same as in Tables 4 and 5 but packing height was increased to 20 m. Figure 8 shows the effect of lean loading in solvent capacity. Figure 9 presents the corresponding change in rich loading.

In both figures the optimum curve and the $Z/Z_{\text{Total}} = 0.5$ curve overlap along the studied range. Thus, the position of the intercooling stage is not critical with 20 m of packing.

Figures 10 and 11 show that intercooling at high loading lean feed is not very beneficial because there is a limited temperature increase (7°C) in the absorber. The higher solvent flow needed at high lean loading buffers any temperature increase due to reaction. The heat is absorbed by the

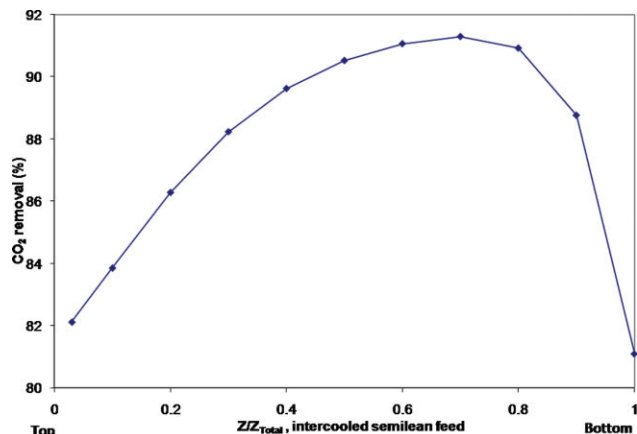


Figure 5. CO_2 removal with intercooled semilean feed for 4.5 m/4.5 m K^+/PZ .

0.5 kPa CO_2 lean solvent, 15 m packing. [Color figure can be viewed in the online issue, which is available at www.interscience.wiley.com.]

increased solvent flow. Thus, mass transfer is not limited by the increase of temperature.

On the other hand, lean loading solvent feeds (Figures 12 and 13) show a large increase in solvent temperature towards the top of the column. The low CO_2 content in the solvent offers an initial high driving force that allows for increased reaction rates at the top of the column causing a noticeable temperature increase. The lower solvent rates are not capable of absorbing all the generated heat and there is a top of column temperature bulge (around 70°C). As temperature increases, the equilibrium becomes a limiting factor; yet, most of the CO_2 has already been absorbed so the bottom of the column does not react much. Figure 13 shows that the use of intercooling does not provide a considerable benefit in performance. The CO_2 rate profile obtained without intercooling (Figure 12) differs little from the former.

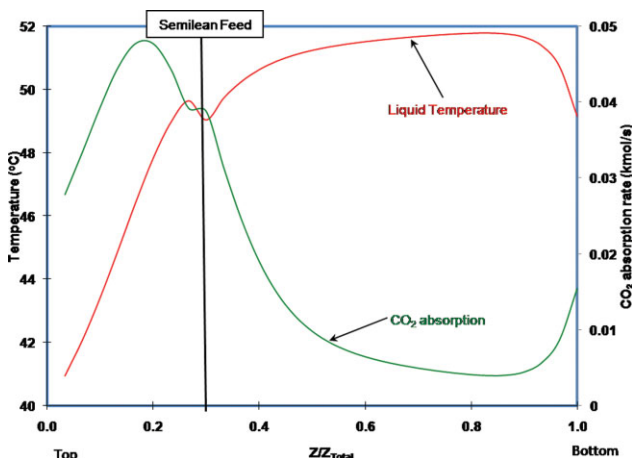


Figure 4. Temperature and CO_2 absorption rate profiles for absorber with semilean feed at 0.30 column height; no intercooling.

Solvent 4.5 m/4.5 m K^+/PZ , 0.5 kPa CO_2 lean solvent, 15 m packing. [Color figure can be viewed in the online issue, which is available at www.interscience.wiley.com.]

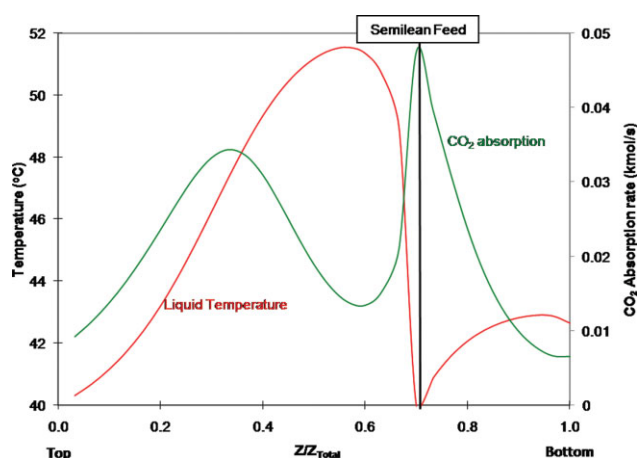


Figure 6. Temperature and CO_2 rate profiles for absorber with intercooled semilean feed at 0.70 column height.

Solvent 4.5 m/4.5 m K^+/PZ , 0.5 kPa CO_2 lean solvent, 15 m packing. [Color figure can be viewed in the online issue, which is available at www.interscience.wiley.com.]

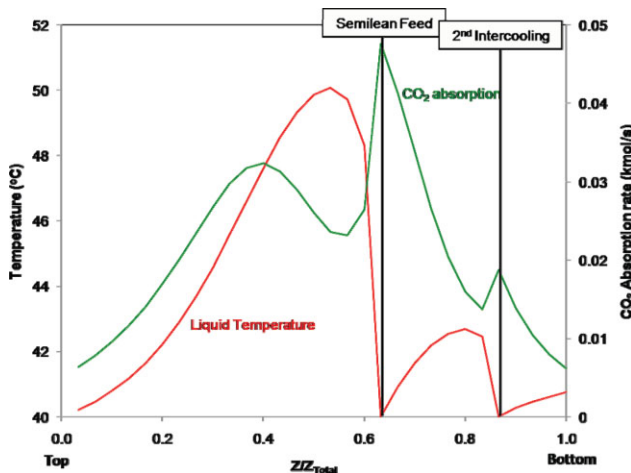


Figure 7. Temperature and CO_2 rate profiles for absorber with intercooled semilean feed at 0.63 and intercooling at 0.87 column height.

Solvent 4.5 m/4.5 m K^+ /PZ, 0.5 kPa CO_2 lean solvent 15 m packing. [Color figure can be viewed in the online issue, which is available at www.interscience.wiley.com.]

However, absorbers operating at conditions within the loading bracket 0.27–0.40 mol CO_2 /mol alkalinity benefit from intercooling. The temperature bulge is located near the center of the column and limits mass transfer rates. By adding intercooling, it is possible to boost this phenomenon thanks to a lowering of the temperature of the bulge and of the column in general. (See Figures 14 and 15) This bracket is defined as the critical L/G region.

Looking at the behavior of the rich loading with respect to lean loading (Figure 9), intercooling proves especially beneficial between in the critical L/G (0.27–0.40 mol CO_2 /mol alkalinity) for stripper performance. The higher loading from the absorber allows for lower energy consumption in the stripper.

Determining the Critical Liquid–Gas Ratio (L/G_c)

The benefit of using intercooling is maximized when the selected operating conditions cause the temperature bulge to coincide with a mass transfer pinch. This relates to the capacity of the gas and the liquid to carry heat out of the column. At the critical L/G the heat generated by the absorption of CO_2 is removed evenly between the liquid and the gas producing a temperature bulge towards the middle of the column.

In order to determine the critical L/G it is useful to set up global mass and energy balances and balances between the top of the column and the location of the temperature bulge. The global energy balance can be written as follows:

Table 6. CO_2 Removal Results for K^+ /PZ Absorber Configurations

CO ₂ Pressure in Lean Solvent @ 40°C	0.5 kPa	0.7 kPa
Intercooling	CO ₂ Removal (%)	
None	81.4	71.6
Single with semilean feed	91.3	82.9
Double	92.8	84.2

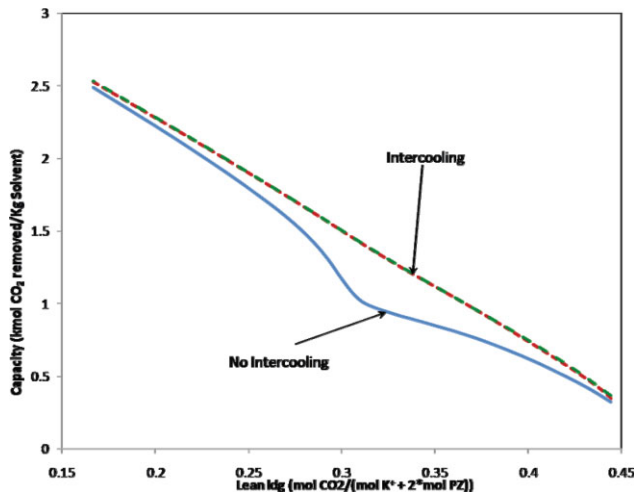


Figure 8. Change in solvent capacity vs. lean loading.

4.5 m K^+ /4.5 m PZ, 90% CO_2 removal with 20 m of CMR#2 packing. [Color figure can be viewed in the online issue, which is available at www.interscience.wiley.com.]

$$L_{\text{in}}H_{\text{in}}^{\text{L}} + G_{\text{in}}H_{\text{in}}^{\text{G}} = L_{\text{out}}H_{\text{out}}^{\text{L}} + G_{\text{out}}H_{\text{out}}^{\text{G}} \quad (8)$$

where: L and G are the liquid and gas flow rates, respectively, (moles/s); H is the enthalpy of the stream; ^{L,G} are superscripts for gas and liquid properties; _{in, out} label inlet and outlet streams around the absorber.

Likewise, an energy balance around the top of the absorber and the location of the temperature bulge results in the following equality:

$$L_{\text{in}}H_{\text{in}}^{\text{L}} + G_{\text{b}}H_{\text{b}}^{\text{G}} = L_{\text{b}}H_{\text{b}}^{\text{L}} + G_{\text{out}}H_{\text{out}}^{\text{G}} \quad (9)$$

where _b stands for conditions at the temperature bulge location.

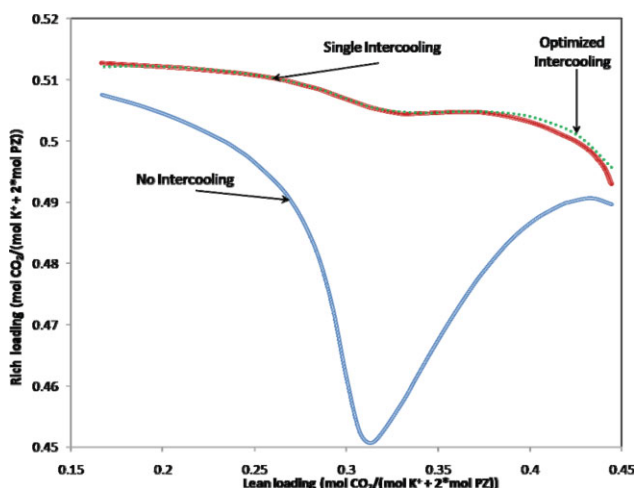


Figure 9. Variation of rich loading with lean loading.

4.5 m K^+ /4.5 m PZ, 90% CO_2 removal with 20 m of CMR#2 packing. [Color figure can be viewed in the online issue, which is available at www.interscience.wiley.com.]

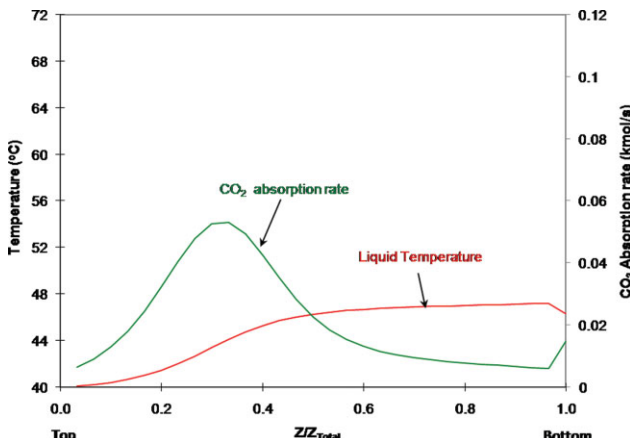


Figure 10. Temperature and CO₂ rate profiles for absorber.

4.5 m K⁺/4.5 m PZ with a lean loading of 0.44. [Color figure can be viewed in the online issue, which is available at www.interscience.wiley.com.]

The following approximations and assumptions will be made to determine (L/G)_c based on engineering criteria and observations from the presented modeling cases:

- In the global energy balance enthalpies are determined using the inlet liquid temperature (T_{in}^L) as reference temperature (T_0). This eliminates the inlet liquid term from Eq. 8.
- The energy contribution due to CO₂ absorption and vaporization of water is included in the outlet gas enthalpy as follows:

$$G_{out}H_{out}^G = G_{out}Cp_{out}^G(T_{out}^G - T_0) + \left(n_{out}^{CO_2(g)} - n_{in}^{CO_2(g)} \right) h_{abs}|_{T_0} + \left(n_{out}^{H_2O(g)} - n_{in}^{H_2O(g)} \right) h_{vap}|_{T_0} \quad (10)$$

where: n is the flow rate (moles/s) of CO₂ or H₂O, respectively, in the gas; T_0 is the reference temperature; $h_{abs}|_{T_0}$ is

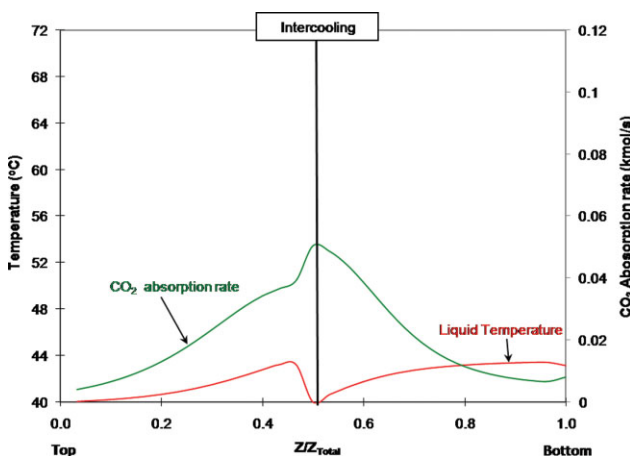


Figure 11. Temperature and CO₂ rate profiles for absorber with intercooling at 0.50 column height.

4.5 m K⁺/4.5 m PZ with a lean loading of 0.44. [Color figure can be viewed in the online issue, which is available at www.interscience.wiley.com.]

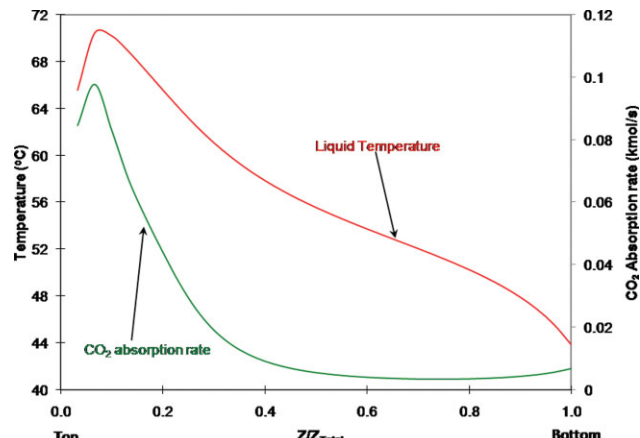


Figure 12. Temperature and CO₂ rate profiles for absorber.

4.5 m K⁺/4.5 m PZ with a lean loading of 0.21. [Color figure can be viewed in the online issue, which is available at www.interscience.wiley.com.]

the CO₂ heat of absorption at T_0 ; $h_{vap}|_{T_0}$ is the heat of vaporization of water at T_0 ; Cp_{out}^G is the heat capacity of the gas at outlet conditions.

- Replacing Eq. 10 in the global energy balance and including the expressions for outlet liquid and inlet gas enthalpy results in:

$$G_{out}Cp_{out}^G(T_{out}^G - T_{in}^L) + \left(n_{out}^{CO_2(g)} - n_{in}^{CO_2(g)} \right) h_{abs}|_{T_{in}^L} + \left(n_{out}^{H_2O(g)} - n_{in}^{H_2O(g)} \right) h_{vap}|_{T_{in}^L} + L_{out}Cp_{out}^L(T_{out}^L - T_{in}^L) = G_{in}Cp_{in}^G(T_{in}^G - T_{in}^L) \quad (11)$$

where: Cp_{out}^L , is the heat capacity of the liquid at outlet conditions;

Cp_{in}^G is the heat capacity of the gas at inlet conditions.

- We have observed from simulations that the maximum temperature at the bulge is approximately equal to the

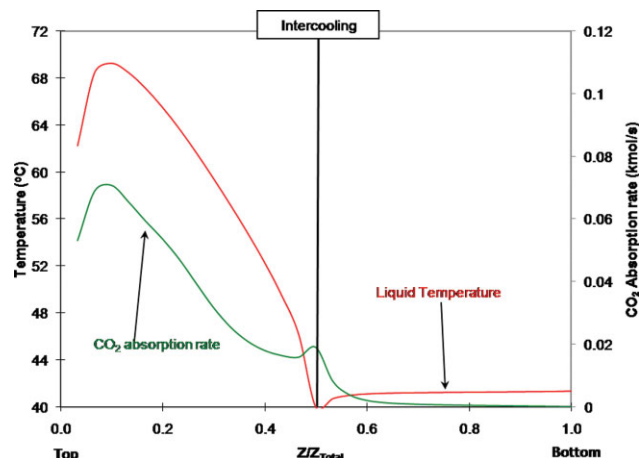


Figure 13. Temperature and CO₂ rate profiles for absorber with intercooling at 0.50 column height.

4.5 m K⁺/4.5 m PZ with a lean loading of 0.21. [Color figure can be viewed in the online issue, which is available at www.interscience.wiley.com.]

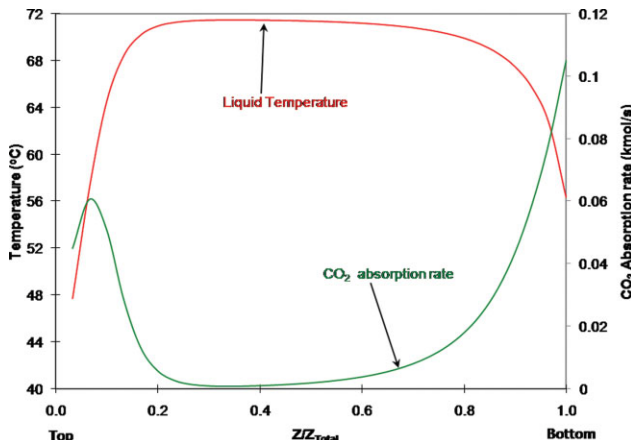


Figure 14. Temperature and CO₂ rate profiles for absorber.

4.5 m/4.5 m K⁺/PZ with a lean loading of 0.315. [Color figure can be viewed in the online issue, which is available at www.interscience.wiley.com.]

temperature that the gas would have if all of the heat of absorption were carried out with the gas. The global energy balance (Eq. 11) for a system in which all the heat leaves with the gas out the top of the absorber ($T_{\text{out}}^{\text{L}} = T_{\text{in}}^{\text{L}}$) is reduced to:

$$G_{\text{out}} C p_{\text{out}}^{\text{G}} (T_{\text{out}}^{\text{G}} - T_{\text{o}}) + \left(n_{\text{out}}^{\text{CO}_2(\text{g})} - n_{\text{in}}^{\text{CO}_2(\text{g})} \right) h_{\text{abs}}|_{T_{\text{o}}} + \left(n_{\text{out}}^{\text{H}_2\text{O}(\text{g})} - n_{\text{in}}^{\text{H}_2\text{O}(\text{g})} \right) h_{\text{vap}}|_{T_{\text{o}}} = 0 \quad (12)$$

The right side of Eq. 12 is set to zero because for all of the cases the inlet liquid temperature was set equal to the gas inlet temperature (40°C).

- By defining a desired removal (R) the outlet gas water content is calculated. Assuming that the outlet gas leaves in equilibrium with the inlet solvent it is possible to determine

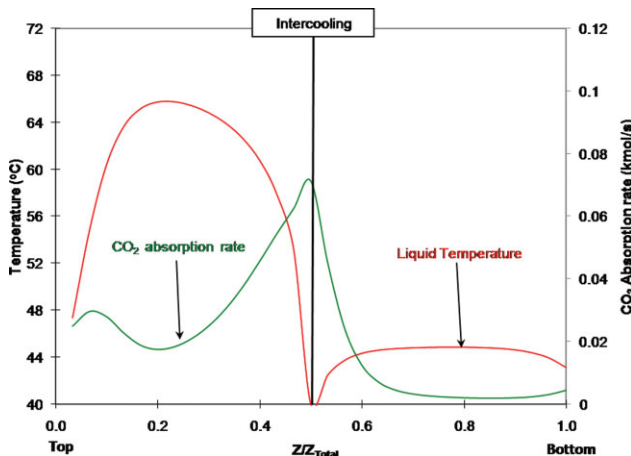


Figure 15. Temperature and CO₂ rate profiles for absorber with intercooling at 0.50 column height.

4.5 m/4.5 m K⁺/PZ with a lean loading of 0.315. [Color figure can be viewed in the online issue, which is available at www.interscience.wiley.com.]

the outlet temperature using equations of state or steam tables. This value is used as an approximation to the bulge temperature (T_b):

$$\left(\frac{n_{\text{out}}^{\text{H}_2\text{O}}}{G_{\text{out}}} \right) P_{\text{Total}} = \frac{y_{\text{out}}^{\text{H}_2\text{O}}}{x_{\text{in}}^{\text{H}_2\text{O}}} P_{\text{Total}} = P_{\text{sat}}^{\text{H}_2\text{O}} = f(T) \quad (13)$$

Here, the outlet gas flow (G_{out}) is calculated using the inlet gas composition and taking into account the outlet water content and the removed carbon dioxide. $x_{\text{in}}^{\text{H}_2\text{O}}$ is the mole fraction of water in the inlet solvent.

- If in Eq. 9 the reference temperature (T_o) is set to the bulge temperature (T_b) the resulting energy balance is:

$$L_{\text{in}} C p_{\text{in}}^{\text{L}} (T_{\text{in}}^{\text{L}} - T_b) + \left(n_{\text{out}}^{\text{CO}_2(\text{g})} - n_{\text{b}}^{\text{CO}_2(\text{g})} \right) h_{\text{abs}}|_{T_b} + \left(n_{\text{out}}^{\text{H}_2\text{O}(\text{g})} - n_{\text{b}}^{\text{H}_2\text{O}(\text{g})} \right) h_{\text{vap}}|_{T_b} = G_{\text{out}} C p_{\text{out}}^{\text{G}} (T_{\text{out}}^{\text{G}} - T_b) \quad (14)$$

- The change in liquid flow rate across the column is neglected and the gas flow rate is defined as:

$$G = G^{\text{i}} + n^{\text{CO}_2(\text{g})} + n^{\text{H}_2\text{O}(\text{g})} \quad (15)$$

Here G^{i} represents the inert species present in the gas stream: oxygen and nitrogen

- Introducing Eq. 15 into Eq. 14 and after some manipulation:

$$\left(\frac{L}{G_i} \right)_c = (1 + (1 - R) Y_{\text{in}}^{\text{CO}_2} + Y_{\text{out}}^{\text{H}_2\text{O}}) \left(\frac{C p_{\text{out}}^{\text{G}}}{C p_{\text{in}}^{\text{L}}} \right) + \frac{(Y_b^{\text{CO}_2} - (1 - R) Y_{\text{in}}^{\text{CO}_2}) n_{\text{abs}}|_{T_b} + (Y_{\text{out}}^{\text{H}_2\text{O}} - Y_b^{\text{H}_2\text{O}}) n_{\text{vap}}|_{T_b}}{C p_{\text{in}}^{\text{L}} (T_{\text{in}}^{\text{L}} - T_b)} \quad (16)$$

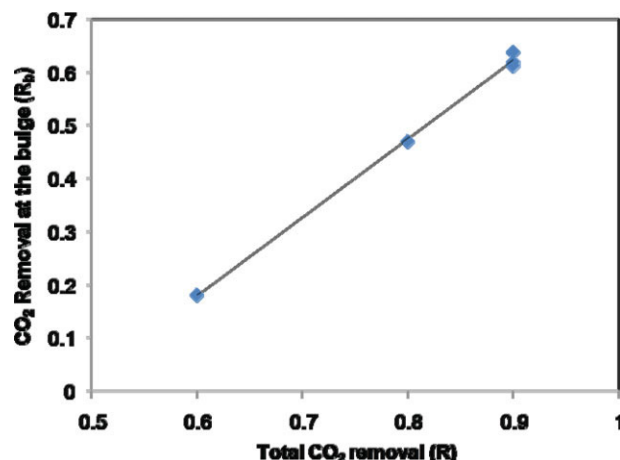


Figure 16. CO₂ removal at the bulge as a function of total removal.

Points are simulation results. All cases with 10 m packing height. For 90% removal two additional points are included at 20 m and 5 m of packing. [Color figure can be viewed in the online issue, which is available at www.interscience.wiley.com.]

Table 7. Temperature Bulge and Critical L/G Predictions. Variable Packing and Removal

Packing Height (m)	CO ₂ Removal (%)		(L/G) _c		T _b (°C)		y _{out} ^{H₂O}		T _{out} ^G (°C)	
	Total	Below Bulge	Aspen	Approx	Aspen	Approx	Aspen	Approx	Aspen	Approx
5	90	61.9	3.9	4.0	69	68	0.09	0.06	46	40
10	90	63.8	4.1	4.0	72	68	0.10	0.06	46	40
20	90	61.2	4.1	4.0	72	68	0.09	0.06	46	40
10	80	47.0	3.8	4.1	69	66	0.10	0.06	48	40
10	60	18.1	3.5	4.5	61	62	0.09	0.06	47	40

where: $(L/G)_c^i$ is the critical ratio of liquid to inert gas species; $y_{out}^{H_2O}$, $y_{in}^{H_2O}$ are the fractions of water and carbon dioxide, respectively, to inert species in the gas stream (n_{CO_2}/G_i^i , n_{H_2O}/G_i).

- The outlet gas water content can be calculated using an equilibrium relation:

$$y_{out}^{H_2O} = x_{in}^{H_2O} P_{sat}^{H_2O}(T_{in}^L) \quad (17)$$

where: $y_{out}^{H_2O}$, $x_{in}^{H_2O}$ are mole fractions of water in the gas and liquid; $P_{sat}^{H_2O}$ is the vapor pressure of water at the inlet liquid temperature (T_{in}^L).

- The CO₂ content at the temperature bulge is approximated based on results for simulations at various removals. Figure 16 gives total CO₂ removal as a function of the removal obtained at the bulge. Results fit the following equation depending only on the desired final removal:

$$R_b = 1.4728R - 0.7038 \quad (18)$$

where R_b is the removal at the bulge. Equation 18 fits the data adequately independent of the packing height used.

It is worth noticing that Eq. 16 is independent of the height of packing and was generated from simple energy and heat balances. Its validation was done at constant removal (R) varying the height of packing, and at constant packing height but variable removal (Table 7).

The proposed approximation gives a relatively good estimate of the critical L/G (less than 10% deviation) for all cases except at 60% removal. As for the temperature bulge, it is adequately predicted with a maximum deviation of 4°C.

Conclusions

Absorber intercooling increases CO₂ removal by as much as 10% in the double matrix example. Adequate positioning of the intercooled semilean feed and the additional intercooling assures the best possible performance of the column in this configuration.

In simple absorbers where the temperature of the solvent is increased by heat of absorption, as with the K⁺/PZ system, intercooling appears beneficial if the temperature bulge is located toward the middle of the column and coincides with a mass transfer pinch (critical L/G). In this case, it will allow for higher absorption by reducing the magnitude of the bulge temperature and increasing solvent capacity by as much as 45%. Additionally, intercooling will offer a benefit

in energy consumption in the stripper because of the richer feed from the absorber. However, for systems with low L/G where the bulge is located towards the top of the column and away from the mass transfer pinch, intercooling will offer limited improvement. In the same way, with high L/G the temperature bulge is small and its location matches the pinch at the bottom of the column, so intercooling will also offer very limited enhancement. In both cases, intercooling may prove to be impractical because of capital costs required for its implementation.

An approximation of the critical L/G for the absorption of CO₂ has been developed. It requires knowledge of the heat of absorption of the solvent and approximate values for the heat capacities of the gas and the liquid. Its accuracy is strongly dependent on the estimation of the CO₂ content at the temperature bulge. For the expected operating removal (>80%), it is capable of calculating (L/G)_c with less than 10% error for the K⁺/PZ system. The temperature bulge can also be predicted to 4°C.

This approximation also gives some insight into the possible behavior of the critical L/G with different solvents. A solvent with a heat of absorption 30% lower than the studied K⁺/PZ will result in a 15% lower critical L/G. Similarly, a solvent with a heat of absorption 30% higher will result in a 15% higher critical L/G.

The developed approximation may prove to be a valuable tool when optimizing lean loading operation since it gives an idea of conditions to avoid where intercooling is not an option, without running any simulation models.

Literature Cited

- Jackson RM, Sherwood TK. Performance of Refinery gas absorbers with and without intercoolers. *Am Inst Chem Eng Trans.* 1941; 37:959–978.
- Linhoff HR. Intercoolers used in absorber at vapor-recovery plants. *Natl Pet News.* 1930;22:20.
- Sobel BA. Iterative processes: a relaxation operator and its application to the computation of absorber columns. *Am Chem Soc Div Pet Chem.* 1968;13:5.
- Thompson RE, King CJ. Energy conservation in regenerated chemical absorption processes. *Chem Eng Process.* 1987;21:14.
- Chang H, Shih CM. Simulation and optimization for power plant flue gas CO₂ absorption-stripping systems. *Sep Sci Technol.* 2005;40:877–909.
- Tobiesen FA, Svendsen HF, Mejell T. Modeling of blast furnace CO₂ capture using amine absorbents. *Ind Eng Chem Res.* 2007; 46:7811–7819.
- Freguia S, Rochelle GT. Modeling of CO₂ capture by aqueous monoethanolamine. *AIChE J.* 2003;49:1676–1686.
- Mark S. Purification and separation of gaseous mixtures. United States Patent Office. Patent Number: 1971798, 1934.

9. Geleff S. Method and device for recovery of thermal energy from an exothermic carbon dioxide absorption process. WO/2003/028854, 2003.
10. Reddy S, Scherffius J, Gilmartin J, Freguia S. Split flow process and apparatus. WO/2004/005818, 2006.
11. Kvamsdal HM, Rochelle GT. Effects of the temperature bulge in CO₂ absorption from flue gas by aqueous monoethanolamine. *Ind Eng. Chem. Res.* 2008;47:867–875.
12. Chen E. *Carbon Dioxide Absorption into Piperazine Promoted Potassium Carbonate using Structured Packing*. Ph.D. Dissertation, The University of Texas at Austin, Austin, Texas, 2007.
13. Cullinane JT. *Thermodynamics and Kinetics of Aqueous Piperazine with Potassium Carbonate for Carbon Dioxide Absorption*. Ph.D. Dissertation, The University of Texas at Austin, Austin, Texas, 2005.
14. Hilliard M. *Thermodynamics of Aqueous Piperazine/Potassium Carbonate/Carbon Dioxide Characterized by the Electrolyte NRT Model within Aspen Plus®*. Masters Dissertation, The University of Texas at Austin, Austin, Texas, 2005.
15. Bishnoi S, Rochelle GT. Absorption of carbon dioxide in aqueous piperazine/methyldiethanolamine. *AIChE J.* 2002;48:2788–2799.
16. Onda K, Takeuchi H, Okumoto Y. Mass transfer coefficients between gas and liquid phases in packed columns. *J Chem Eng Jpn.* 1968;1:56–52.
17. Oyenekan BA, Rochelle GT. Alternative stripper configurations for CO₂ capture by aqueous amines. *AIChE J.* 2007;53:3144–3154.
18. Rochelle G, Seibert F, Closmann F, Cullinane JT, Davis J, Goff G, Hilliard M, McLees J, Plaza JM, Sexton A, Van Wagenen D, Xu Q, Veawab A, Nainar M. *CO₂ Capture by Absorption with Potassium Carbonate*. The University of Texas at Austin, Austin, Texas, DE-FC26-02NT41440; 2007.

Manuscript received Feb. 25, 2009, and revision received July 14, 2009.